

A 100KHz-1GHz Termination-dependent Human Body Communication Channel Measurement using Miniaturized Wearable Devices

Shitij Avlani, Mayukh Nath, Shovan Maity, *Member, IEEE*, and Shreyas Sen, *Senior Member, IEEE*

Abstract—Human Body Communication has shown great promise to replace wireless communication for information exchange between wearable devices of a body area network. However, there are very few studies in literature, that systematically study the channel loss of capacitive HBC for *wearable devices* over a wide frequency range with different terminations at the receiver, partly due to the need for *miniaturized wearable devices* for an accurate study. This paper, for the first time, measures the channel loss of capacitive HBC from 100KHz to 1GHz for both high-impedance and 50Ω terminations using wearable, battery powered devices; which is mandatory for accurate measurement of the HBC channel-loss, due to ground coupling effects. Results show that high impedance termination leads to a significantly lower channel loss (40 dB improvement at 1MHz), as compared to 50Ω termination at low frequencies. This difference steadily decreases with increasing frequency, until they become similar near 80MHz. Beyond 100MHz inter-device coupling dominates, thereby preventing accurate measurements of channel loss of the human body. The measured results provide a consistent wearable, wide-frequency HBC channel loss data and could serve as a backbone for the emerging field of HBC by aiding in the selection of an appropriate operation frequency and termination.

Index Terms—Human Body Communication (HBC), Body Coupled Communication (BCC), channel measurements

I. INTRODUCTION

The exponential scaling of transistors has enabled the production of wearable devices for fitness monitoring, medical diagnosis, and other applications. These devices are usually interconnected to relay sensor readings and other data, creating a local network known as Body Area Network (BAN). The human anatomy requires these devices to have a small form factor, thereby limiting battery capacity [1] and necessitating ultra-low-power (ULP) circuits. Communication system such as Bluetooth is a significant portion (\sim mW) of the power-budget of such energy-constrained devices. Human body communication (HBC) promises ULP (\sim 10's of μ W) BAN communication by utilizing the conductivity properties of the human body. Therefore, the power benefits similar to wire-line communication [2], [3] can be achieved while keeping the devices physically wireless.

Capacitive HBC involves coupling and receiving the communication signal to the body through a single electrode with a floating ground electrode both at transmitter and receiver. Only

This work was supported by the Air Force Office of Scientific Research YIP Award under Grant FA9550- 17-1-0450 and NSF CRII Award CNS 1657455.

The authors are with the School of Electrical and Computer Engineering, Purdue University, West Lafayette, IN 47907, USA (e-mail: shreyas@purdue.edu)

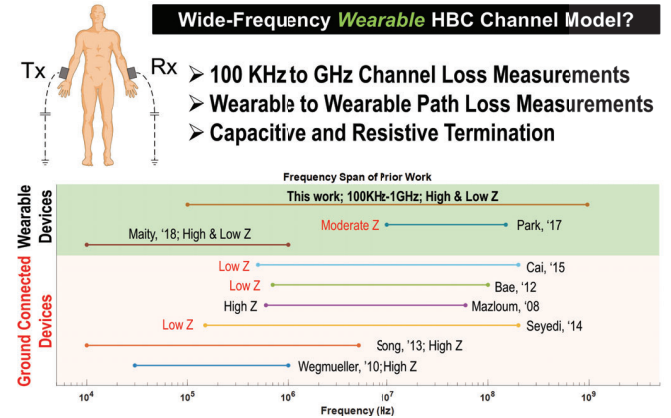


Fig. 1. Frequency-range, termination modality and ground connection used by prior work in HBC channel measurement and the research need [4]–[10]

a few studies on characterizing the channel exist in literature (Fig. 1) on channel which are conducted in a methodical manner and cover a wide range of frequencies with different kinds of termination.

Maity [5] demonstrated that in capacitive-voltage mode HBC with high-impedance termination, the forward path contributed a path loss of only 0.5 dB, indicating that the return path capacitance primarily controls channel loss, later analyzed in-depth by Nath [11]. Traditionally, path loss measurements were made using ground connected devices such as vector network analyzers, which short the return path capacitance and grossly underestimate the path loss. Subsequently, a balun was placed between the electrodes and the measurement device to prevent this [6], [10]. Although this was a step in the right direction, the channel loss measurements were still optimistic due to large ground plane and large return path capacitance. These results obtained from large, ground connected devices are invalid for miniaturized wearable devices.

Maity developed the first Bio-Physical model [4] which established the underlying mechanism of low-frequnecy capacitive HBC as electro-quasistatic transport [3] and described the channel characteristics for various parameters like single-ended and differential electrodes, ground connected and wearable devices, among others. Although this paints a vivid picture of the channel characteristics, with both high-impedance capacitive and resistive termination, the frequency range was limited till only 1 MHz. Park [7] developed miniature wearable devices to measure channel loss from 10 MHz to 150 MHz,

using moderate impedance matching networks to maximize the power transfer. This is not the optimal choice for a voltage signaling based communication, especially at low frequencies.

Maity and Park are the only studies to utilize wearable devices for channel loss measurements. However, they investigate dissimilar parameters i.e. a small span of frequency and one kind of termination. Therefore, it is imperative to present a unified set of measurements using wearable devices over wide-frequency range to help optimize HBC transceivers.

II. BIO-PHYSICAL MODEL

The bio-physical model proposed by Maity [4] for capacitive HBC is shown in Fig. 2a. The underlying mechanism for low frequencies is approximated as electro-quasistatic transport since the signal wavelength is an order of magnitude larger than the body dimension. Discounting a 5% error, this approximation is valid roughly up to 10MHz [3].

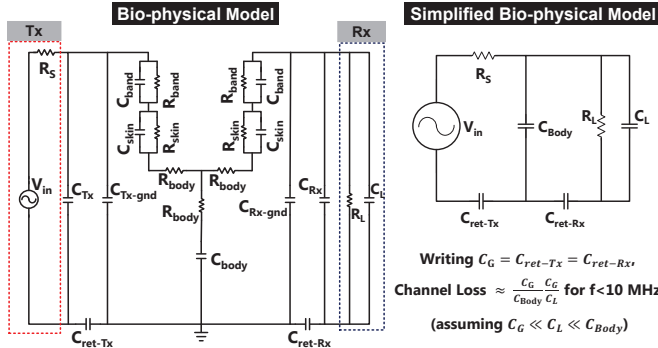


Fig. 2. (a) Biophysical model [4]; (b) Simplified biophysical model [11].

The bio-physical model explains the various resistances and parasitic capacitance associated with HBC. The transmitter is modelled as a voltage source with a small series source impedance, whereas the receiver is modelled by its termination impedance. The return path capacitance between earth's ground and the communication devices' floating ground closes the circuit loop, allowing signal transmission. Parasitic capacitances between the earth's ground and the body, and those between the body and communication devices further affect the signal transmission and channel loss.

The return path capacitance and load capacitance primarily dictates the overall channel loss of EQS-HBC. Hence, the bio-physical model could be simplified as shown in Fig.2b, [11]. The return path capacitance (C_G) could be approximated as the self-capacitance and is proportional to the ground plane size of the transmitter and receiver [11], increasing loss for a lower (C_G) (i.e. smaller device) or a higher load capacitance (C_L). Hence, to measure channel loss for wearable devices, small form factor measurement devices must be used.

At high frequencies (beyond 10MHz), the mechanism for HBC transitions from electro-quasistatic transport to electromagnetic. As the return path capacitance will continue to play a role during this transition, a small device is still imperative for high frequency measurements. Additionally, the small size will help reduce inter-device coupling.

As shown in Fig. 2, the termination impedance of the receiver significantly affects channel loss in HBC. Therefore, correct termination at the receiver is of utmost importance. Previous studies [4] have shown that 50Ω termination should be avoided at low frequencies. However, as frequency increases the input impedance seen at the receiver will decrease and may eventually fall below 50Ω . It is possible that a 50Ω terminated receiver could exhibit a lower channel loss at high frequencies. Therefore the optimal termination at high frequency should be investigated in the future. Here we measure wide-frequency channel loss with wearable devices for both 50Ω and high-impedance termination (C_L).

III. MEASUREMENT SETUP

A. Measurement Location: Anechoic Chamber

All path loss measurements are conducted inside an anechoic chamber to prevent multi-path effects and external interference from influencing the readings. The chamber has a dimension of 400x550x400 cm and the inner walls are lined with a spike-patterned foam which efficiently absorb electromagnetic waves above 80MHz. As depicted in Fig. 3, the human subject was placed the centre of the room to maximize distance from the side walls which are connected to earth's ground. This will minimize the change in return capacitance and accurate path loss values can be obtained.

B. Setup: Wearable Signal Transmitter

The entire frequency range could not be covered by a single off-the-shelf, wearable, battery powered signal generator. Therefore, two devices (Fig. 4a) were used as the transmitter, one for low frequency and the other for high frequency.

1) Low-Frequency (100KHz to 20MHz): The EK-TM4C123GXL launchpad by Texas Instruments which highlights the TM4C123GH6PM micro-controller is used as the low frequency transmitter. It is powered by a small battery and placed in a 3D printed enclosure. The coupling electrode is made from copper tape which is fixed to an elastic band. The electrode is connected to one of the GPIO pins of the micro-controller which generates a PWM signal. The micro-controller is programmed to generate a PWM signal of 3.3V with a duty cycle of 50% between 100KHz and 20MHz. Two switches on the PCB which were programmed to cycle through the required PWM frequencies.

2) High-Frequency (24MHz to 960MHz): A handheld RF signal generator (RFE6GEN) from RF Explorer is used as the transmitter for the high frequency range. The device dimension is 113x70x25 mm, and operates between 24MHz to 6GHz with a resolution of 1KHz and a frequency stability of 0.5ppm. The output signal power is 0dBm at 50Ω , with an accuracy of +/- 3dB. The device body is made of aluminum and is connected to ground, therefore a layer of foam is connected below the device to prevent the body from touching the ground plane of the device.

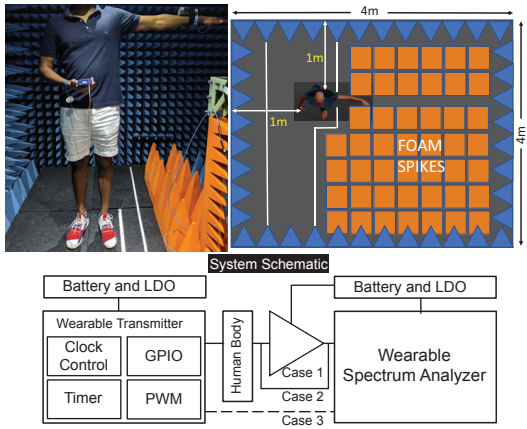


Fig. 3. (a) Body posture for which measurements were collected; (b) Animation depicting the anechoic chamber and the physical location at which the measurements were conducted; (c) System schematic.

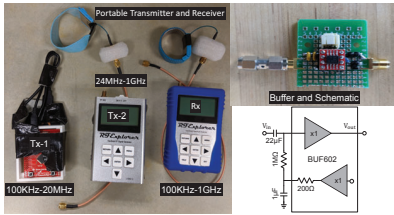


Fig. 4. (a) Low and high frequency transmitter and receiver used for measurements; (b) High frequency buffer and schematic.

C. Setup: Wearable Signal Receiver

A handheld RF spectrum analyzer (WSUB1G+) from RF Explorer is used as the wearable receiver for the entire frequency range (Fig. 4a). The device operates between 100KHz to 960MHz with a resolution of 0.5dB and an average noise level and amplitude accuracy of -125dB and +/-3dB, respectively. The device body is again made of aluminum and connected to ground, therefore the protective measures described above are used. The receiver has an input impedance of 50Ω . For low impedance termination measurements, the coupling electrode band was directly connected to the input SMA port (CASE 2 in Fig. 3c). For high impedance measurements, a buffer was connected (CASE 1) between the electrode and the input of the receiver.

D. Buffer for High Impedance Termination

The high bandwidth buffer circuit was assembled on a perforated board. A high-speed buffer IC, BUF602 from Texas Instruments was used. It has a wide bandwidth of 1GHz, a slew rate of $8000V/\mu s$, and an internal reference voltage generator, which is perfect for buffering the transmitted high-speed AC signal. The input impedance of the buffer is $1M\Omega$ with a capacitance of $2.1pF$. The input capacitance (C_L) of the complete receiver will determine the measurement and will change according to the formula shown in Fig. 2b.

E. Inter-device Coupling

Inter-device coupling measurements (CASE 3, dashed line implies no physical connection) were performed by suspend-

ing the devices inside the anechoic chamber at the exact same location as they would be if a human subject was wearing them, such that the devices see similar parasitic capacitance, making the human body as the only variable in the setup. However, practically realizing the exact same orientation for all measurements proved to be difficult, which resulted in a high variance for inter-device coupling measurements (Fig. 6).

IV. MEASUREMENTS AND ANALYSIS

A. Measurement Procedure

Standardized procedure was developed and repeated, since channel loss measurements are susceptible to variations. The subject was placed at the exact same location in the anechoic chamber. The transmitter was tied to the left hand which was outstretched at shoulder, and the receiver was placed in the right hand in front of the belly. The orientation of the electrode bands were kept consistent and great care was taken to ensure a steady body posture while collecting the readings.

Due to involuntary variations in posture and placement of devices resulting from human error, fluctuations in the readings were inevitable. This was addressed by repeating the measurements multiple times over the course of a few days and averaging the results. The measurements were carried out until the standard deviation of the results dropped below 3dB. This was achieved for high frequency and low frequency channel loss measurements after 10 and 3 repetitions, respectively. Each measurement involved collecting data for both 50Ω and high impedance terminations.

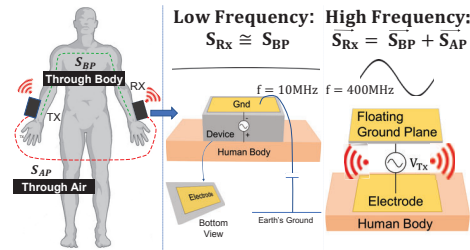


Fig. 5. Physical path of the transmitted signal at low-frequency (mostly body) and high frequency (body and air)

High frequency measurements were carried out at 25 equally spaced points in the logarithmic scale between 24MHz and 960MHz. The transmitter was operated at power level 4, which generated a signal power between 0.1dBm and 1dBm at the fundamental frequency. Since voltage mode signaling is used in capacitive HBC, the power levels were converted to voltage before calculating channel loss. The transmitted signal power values were converted to peak voltage by, $V_{peak-Tx} = 2 * 10^{\frac{P_{Tx,dBm}-10}{20}}$. The receiver recorded the input signal power at the fundamental frequency. Since the wearable spectrum analyzer has an input impedance of 50Ω , the recorded signal power can be converted to peak voltage by, $V_{peak-Rx} = 10^{\frac{P_{Rx,dBm}-10}{20}}$ and the resulting channel loss is given by, $ChannelLoss = 20 * Log_{10}(\frac{V_{peak-Rx}}{V_{peak-Tx}})$.

Low frequency measurements were carried out at 32 equally spaced points in the logarithmic scale between 100KHz and

20MHz. The peak voltage at the fundamental frequency of the PWM signal was calculated by computing the Fourier Transform. The peak voltage at the receiver and subsequently the channel loss was calculated as described above. For each of these frequency points the inter-device coupling readings were noted. The values below the noise floor were not plotted.

B. Result Analysis and Insights

The average path loss and standard deviation from 100KHz to 1GHz is depicted in Fig. 6. From the graph it is clearly evident that the path loss at low frequencies for 50Ω termination is more than 40dB higher (100KHz) than that for high impedance termination, which is more or less flat up to 10MHz where the difference reduces to 20dB. The flat-band loss is highly dependent on the C_L of the receiver. Beyond 10MHz, the impedance of C_L (*i.e.* $\frac{1}{j\omega C_L}$) starts approaching the resistive termination impedance of 50Ω . Consequently, the difference in the channel loss values reduces. The channel loss of high impedance termination can be further reduced by reducing C_L which is a function of the PCB capacitance and the input capacitance of the buffer. In this case the chosen buffer IC and the perforated PCB used to make the circuit has resulted in a path loss of 60dB, which can be reduced by either using a thicker custom made PCB and/or a different buffer IC.

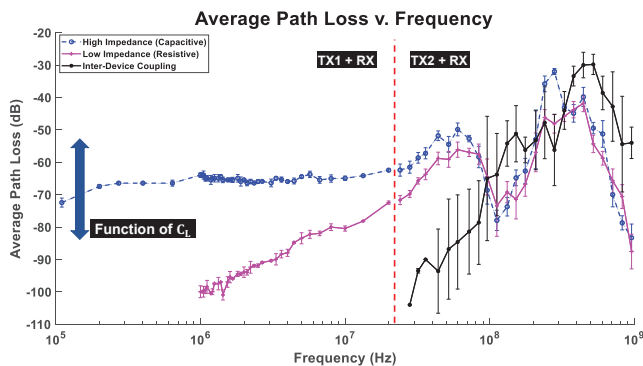


Fig. 6. Wide-frequency Human Body Channel-loss for capacitive HBC with high impedance and resistive termination along with inter-device coupling.

Above 50-100 MHz, there is a low-pass filtering effect formed by R_S and C_L in Fig. 2(b). Additionally, the inter-device coupling starts to play a significant role as the dimensions of the tx/rx devices and coupling electrodes become comparable to the wavelength (Fig. 5). Basically, the coupler electrodes start functioning as a low-Q antenna, and a major part of the transmission takes place through direct electromagnetic radiation between the devices, as opposed to a body-channel mode of communication. Evidently, the transmitted power peaks at about 500 MHz ($\lambda = 60\text{cm}$) which is about 4 times the device dimensions. Also, as seen in Fig 6, the device-device coupling in absence of the human subject can be higher compared to the transmission when the subject is present. This further confirms that the peaking in this region happens because of line-of-sight wireless style transmission, and the human subject being in the way could hurt the transmission.

Accurately characterizing the channel for capacitive HBC at frequencies above 100MHz is in fact complicated since it's extremely difficult to isolate signal power through the body. This can be circumvented if the entire signal can be focused into the human body channel with minimal radiation. However, this is not a trivial problem since the coupling electrode band will act as an antenna. This challenge motivates future research on the design of an optimal coupler or antenna which can focus transmitted signal into the human body channel while minimizing radiation leakage and comparing the result from the above with standalone EM-radiation based coupling.

V. CONCLUSION

Methodical characterization of the human body channel for capacitive HBC using miniaturized wearable devices across a wide 4-decade frequency range with various types of termination is presented, which aims to fill the void in literature and serve as the backbone for the emerging field of HBC. The results have shown that channel loss is significantly higher at low frequencies for a 50Ω termination as compared to high impedance termination. The difference steadily decreases beyond 10MHz and beyond 100MHz, inter-device coupling dominates and an accurate measurement of only human-body portion of the channel loss is hard to obtain. This motivates future research on optimizing the electrode coupler and device design to ensure that the transmitted signal is directed into the human body with minimal radiation leakage for comparison as well as optimal BAN antenna/coupler design purposes.

REFERENCES

- [1] B. Chatterjee *et al.*, "Context-aware intelligence in resource-constrained IoT nodes: Opportunities and challenges," *IEEE Design & Test*, vol. 36, no. 2, pp. 7–40, 2019.
- [2] S. Maity *et al.*, "Bodywire: A 6.3-pJ/b 30-mb/s- 30-db sir-tolerant broadband interference-robust human body communication transceiver using time domain interference rejection," *IEEE Journal of Solid-State Circuits*, vol. 54, no. 10, pp. 2892–2906, 2019.
- [3] D. Das *et al.*, "Enabling covert body area network using electro-quasistatic human body communication," *Scientific reports*, vol. 9, no. 1, p. 4160, 2019.
- [4] S. Maity *et al.*, "Bio-physical modeling, characterization, and optimization of electro-quasistatic human body communication," pp. 1791–1802, June 2019.
- [5] S. Maity *et al.*, "Characterization of Human Body Forward Path Loss and Variability Effects in Voltage-Mode HBC," *IEEE Microwave and Wireless Components Letters*, vol. 28, no. 3, pp. 266–268, Mar. 2018.
- [6] M. H. Sayedi *et al.*, "A novel intrabody communication transceiver for biomedical applications," Ph.D. dissertation, Victoria University, Footscray, VIC, Australia, 2014.
- [7] J. Park *et al.*, "Channel Modeling of Miniaturized Battery-Powered Capacitive Human Body Communication Systems," *IEEE Transactions on Biomedical Engineering*, vol. 64, no. 2, pp. 452–462, Feb. 2017.
- [8] M. S. Wegmueller *et al.*, "Signal Transmission by Galvanic Coupling Through the Human Body," *IEEE Transactions on Instrumentation and Measurement*, vol. 59, no. 4, pp. 963–969, Apr. 2010.
- [9] Y. Song *et al.*, "Review of the Modeling, Simulation and Implementation of Intra-body Communication," *Defence Technology*, vol. 9, no. 1, pp. 10–17, Mar. 2013. [Online]. Available: <http://www.sciencedirect.com/science/article/pii/S2214914713000238>
- [10] J. Bae *et al.*, "The signal transmission mechanism on the surface of human body for body channel communication," *IEEE Transactions on Microwave Theory and Techniques*, vol. 60, no. 3, pp. 582–593, 2012.
- [11] M. Nath *et al.*, "Towards understanding the return path capacitance in capacitive human body communication," *IEEE Transactions on Circuits and Systems II: Express Briefs*, pp. 1–1, 2019.